

Allenylidene to Indenylidene Rearrangement in Cationic *p*-Cymene Ruthenium(II) Complexes: Solvent, Counteranion, and Substituent Effects in the Key Step toward Catalytic Olefin Metathesis

Arianna Antonucci,[†] Mauro Bassetti,^{*,†} Christian Bruneau,[‡] Pierre H. Dixneuf,[‡] and Chiara Pasquini[†]

[†]*Istituto CNR di Metodologie Chimiche, Sezione Meccanismi di Reazione, Dipartimento di Chimica, Università “La Sapienza”, P.le A. Moro 5, I-00185 Roma, Italy*, and [‡]*Organométalliques et Catalyse, Institut Sciences Chimiques de Rennes, UMR 6226 CNRS–Université de Rennes, Campus de Beaulieu, 35042 Rennes, France*

Received July 6, 2010

The reaction of $[(\eta^6\text{-}p\text{-cymene})\text{RuCl}(\text{PCy}_3)][\text{OTf}]$ with $\text{Ph}_2\text{C}(\text{OH})\text{C}\equiv\text{CH}$, at rt in benzene- d_6 or in dichloromethane- d_2 , affords the allenylidene complex $[(\eta^6\text{-}p\text{-cymene})\text{RuCl}(\text{=C=C=CPh}_2)\text{PCy}_3][\text{OTf}]$ (**4a**), which is used *in situ* as a catalyst for the ring-closing metathesis (RCM) reaction of diallyltosylamide. A kinetic study is performed by ^1H NMR spectroscopy in benzene- d_6 and dichloromethane- d_2 . The rates of the olefin metathesis process increase with the concentration of the ruthenium complex, but are independent of the olefin concentration, due to rate-determining transformation of the allenylidene complex. The TOF values are higher in benzene- d_6 than in dichloromethane- d_2 . The spontaneous or thermally induced transformations of the allenylidene complexes $[(\eta^6\text{-}p\text{-cymene})\text{RuCl}(\text{=C=C=CAr}_2)\text{PR}_3][\text{X}]$ (Ar = Ph, X = CF_3SO_3^- (OTf) (**4a**), BF_4^- (**4b**), PF_6^- (**4c**), SbF_6^- (**4d**); X = OTf, Ar = *p*-MeOC₆H₄ (**4e**), Ar = *p*-ClC₆H₄ (**4f**), Ar = *p*-FC₆H₄ (**4g**)), prepared *in situ* from the cationic precursors $[(\eta^6\text{-}p\text{-cymene})\text{RuCl}(\text{PCy}_3)][\text{X}]$ (X = OTf (**8a**), BF_4^- (**8b**), PF_6^- (**8c**), SbF_6^- (**8d**) and the propargylic alcohols $(4\text{-YC}_6\text{H}_4)_2\text{C}(\text{OH})\text{C}\equiv\text{CH}$ (Y = H, OMe, Cl, F), are studied by UV–visible spectroscopy by following the disappearance of the allenylidene moiety $\text{Ru}=\text{C}=\text{C}=\text{CAr}_2$. The allenylidene to indenylidene rearrangement involves attack by the *ortho*-carbon of the aryl rings to the electrophilic allenylidene C_α , to form an intermediate arenium ion, and H-transfer from aryl to C_β . Faster rates are observed in benzene than in dichloromethane in all cases. The first-order rate constants, k_{obs} , for complexes **4a–d** (Ar = Ph) depend on the counteranion nature and decrease in the order $\text{BF}_4^- > \text{OTf} \gg \text{PF}_6^- > \text{SbF}_6^-$ in benzene, while they are insensitive to the counteranion nature in dichloromethane. Measurements performed at different temperatures afford the activation parameters $\Delta H^\ddagger = 22 \pm 2 \text{ kcal mol}^{-1}$ and $\Delta S^\ddagger = -1 \pm 5 \text{ cal mol}^{-1} \text{ K}^{-1}$ for complex **4a** at 18–50 °C and $\Delta H^\ddagger = 24 \pm 1 \text{ kcal mol}^{-1}$ and $\Delta S^\ddagger = 1 \pm 1 \text{ cal mol}^{-1} \text{ K}^{-1}$ for complex **4e** at 25–55 °C. The values of activation entropy, which do not support a rate-determining phosphine dissociation step, and the rate effects of the aryl *p*-substituents are consistent with an early transition state in the C–C bond forming step of the ring-closing process. Rate differences between benzene and dichloromethane are discussed in terms of counteranion interactions in the less polar aromatic solvent. The rates of the allenylidene transformation affect directly the rates of the RCM reaction, as indicated by parallel solvent, proton, counteranion, and aryl substituent effects in the two processes, thus establishing the role of allenylidene–indenylidene rearrangement in the acid-free olefin metathesis.

Introduction

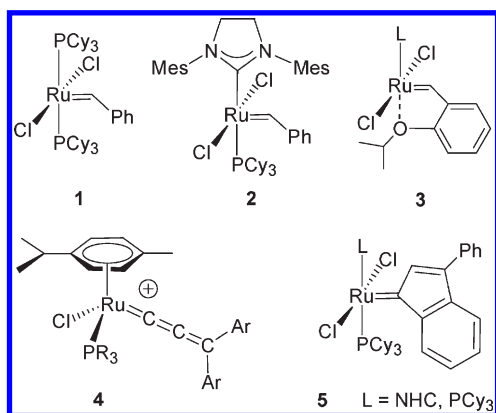
Olefin metathesis represents nowadays one of the most powerful synthetic tools for the transformation and formation of double bonds. This is due to the development of chemically well-defined

metal–alkylidene catalysts, exhibiting efficiency and selectivity along with thermal stability and functional group compatibility.¹ Among various ruthenium-based complexes enabling olefin metathesis reactions, representative structures include the neutral first- and second-generation Grubbs catalysts **1** and **2**, the pyridine-based third-generation catalysts, and the Grubbs–Hoveyda complexes **3** (Chart 1). Continuous efforts have been devoted to modify the catalytic properties of these systems by changes in the metal coordination sphere.² The cationic 18-electron allenylidene ruthenium complexes of general formula $[(\eta^6\text{-}p\text{-cymene})\text{RuCl}(\text{=C=C=CAr}_2)\text{PR}_3][\text{X}]$ (**4**) were also found to promote ring-closing metathesis (RCM) of dienes and enynes,³ as well as ring-opening metathesis polymerization (ROMP) of strained cycloolefins,⁴ thus providing an unprecedented example of the involvement of allenylidenes in alkene metathesis.

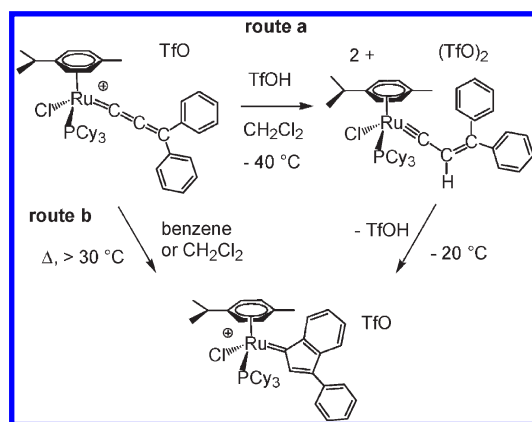
*To whom correspondence should be addressed. E-mail: mauro.bassetti@uniroma1.it.

(1) Reviews: (a) Grubbs, R. H. *Tetrahedron* **2004**, *60*, 7117–7140. (b) Conrad, J. C.; Fogg, D. E. *Curr. Org. Chem.* **2006**, *10*, 185–202. (c) Hoveyda, A. H.; Zhugralin, A. R. *Nature* **2007**, *450*, 243–251. (d) Bielawski, C. W.; Grubbs, R. H. *Progr. Polym. Sci.* **2007**, *32*, 1–29. (e) Clavier, H.; Grell, C.; Kirschning, A.; Mauduit, M.; Nolan, S. P. *Angew. Chem., Int. Ed.* **2007**, *46*, 6786–6801. (f) Schrodi, Y.; Pederson, R. L. *Aldrichim. Acta* **2007**, *40*, 45–52. (g) Hoveyda, A. H.; Malcolmson, S. J.; Meek, S. J.; Zhugralin, A. R. *Angew. Chem., Int. Ed.* **2010**, *49*, 24–44. (h) Voigioukalakis, G. C.; Grubbs, R. H. *Chem. Rev.* **2010**, *110*, 1746–1787.

Chart 1



These allenylidene complexes can be conveniently prepared starting from commercially available ruthenium precursors and propargylic alcohols,^{3a,b,5} a route that stands out as remarkably simple in the crucial context of catalyst synthesis.^{1,2} In terms of activity and selectivity in olefin metathesis reactions, the complex $[(\eta^6\text{-}p\text{-cymene})\text{RuCl}(\text{=C=C=CPh}_2)\text{PCy}_3][\text{OTf}]$ (**4a**, $\text{OTf} = \text{CF}_3\text{SO}_3^-$) was found to correspond to the most efficient combination of phosphine, allenylidene group, and counteranion.^{3a,4a} Significant advancements in understanding the mechanism by which these allenylidene complexes enter the catalytic cycle were obtained from the discovery of the remarkable effect of strong acids on the efficiency of ring-closing and polymerization reactions. It was found that the addition of HBF_4 or TfOH induced the transformation of the allenylidene complex **4a**, via an allenylcarbyne intermediate, into an indenylidene species (Scheme 1, route a), which showed impressive turnover frequencies in the polymerization of cyclooctene and cyclopentene.⁶ In parallel, the formation of an active indenylidene species, although not properly characterized, was postulated to occur upon thermal activation (Scheme 1, route b),

Scheme 1. Rearrangement of the Allenylidene Ruthenium Complex **4a** into the Indenylidene Species, Promoted by Acid (route a) or by Heat (route b)

on the basis of reaction orders and spectroscopic analysis of the RCM of an α,ω -diene substrate.⁷

The remarkable catalytic activity of the neutral indenylidene ruthenium complexes **5**,⁸ with respect to the inertness of the corresponding allenylidene complexes,⁹ further supported the identification of indenylidene derivatives as the key catalytic species. In fact, the coordinatively unsaturated 16-electron $[\text{RuCl}_2(\text{PCy}_3)_2(\text{=C=C=CPh}_2)]$ and $[\text{RuCl}_2(\text{PCy}_3)(\text{IMes})(\text{=C=C=CPh}_2)]$ ($\text{IMes} = 1,3\text{-bis}(2,4,6\text{-trimethylphenyl})\text{imidazol-2-ylidene}$) complexes were stable for days even at 80°C in toluene, thus giving no evidence of allenylidene transformation, and showed in the meantime a poor RCM activity.¹⁰ The efficiency and scope of indenylidene ruthenium(II) complexes of type **5** as olefin metathesis catalysts are currently well documented.¹¹

The acid-induced activation of the allenylidene *p*-cymene complexes was further investigated, and the cationic indenylidene compounds $[(\eta^6\text{-}p\text{-cymene})\text{RuCl}(\eta^1\text{-indenylidene})\text{PR}_3][\text{OTf}]$ ($\text{R} = \text{Cy}$, $i\text{Pr}$, and Ph), previously considered as elusive species, were isolated and fully characterized.¹² An analogous acid-promoted allenylidene–indenylidene transformation has been recently demonstrated starting from the neutral allenylidene complex $[\text{RuCl}_2(\text{PPh}_3)_2(\text{=C=C=CPh}_2)]$.¹³ In contrast, the corresponding thermally induced rearrangement of the cationic *p*-cymene complexes **4** remained poorly understood, in spite of its mechanistic interest and relevance for acid-free catalysis.

We now describe the structural and medium parameters that affect the reaction rates of (i) the RCM reaction mediated by the triflate allenylidene complex and of (ii) the allenylidene to

(2) (a) Wakamatsu, H.; Blechert, S. *Angew. Chem., Int. Ed.* **2002**, *41*, 2403–2405. (b) Conrad, J. C.; Snelgrove, J. L.; Eelman, M. D.; Hall, S.; Fogg, D. E. *J. Mol. Cat. A: Chem.* **2006**, *254*, 105–110. (c) Bienek, M.; Bujok, R.; Cabaj, M.; Luga, N.; Lavigne, G.; Arit, D.; Grela, C. *J. Am. Chem. Soc.* **2006**, *128*, 13652–13653. (d) Colacino, E.; Martinez, J.; Lamaty, F. *Coord. Chem. Rev.* **2007**, *251*, 726–764. (e) Michrowska, A.; Grela, C. *Pure Appl. Chem.* **2008**, *80*, 31–43.

(3) (a) Fürstner, A.; Picquet, M.; Bruneau, C.; Dixneuf, P. H. *Chem. Commun.* **1998**, 1315–1316. (b) Fürstner, A.; Liebl, M.; Lehmann, C. W.; Picquet, M.; Kunz, R.; Bruneau, C.; Touchard, D.; Dixneuf, P. H. *Chem.—Eur. J.* **2000**, *6*, 1847–1857. (c) Fischmeister, C.; Castarlenas, R.; Bruneau, C.; Dixneuf, P. H. *NATO Sci. Ser., II* **2003**, *122*, 23–42. (d) Rigaut, S.; Touchard, D.; Dixneuf, P. H. *Coord. Chem. Rev.* **2004**, *248*, 1585–1601. (e) Malacea, R.; Dixneuf, P. H. In *Metal Vinylidenes and Allenylidenes in Catalysis*; Bruneau, C.; Dixneuf, P. H., Eds.; Wiley-VCH Verlag GmbH & Co.: Weinheim, Germany, 2008; pp 251–277.

(4) (a) Csihony, S.; Fischmeister, C.; Bruneau, C.; Horvath, I. T.; Dixneuf, P. H. *New J. Chem.* **2002**, *26*, 1667–1670. (b) Castarlenas, R.; Sémeril, D.; Noels, A. F.; Demonceau, A.; Dixneuf, P. H. *J. Organomet. Chem.* **2002**, *663*, 235–238. (5) Picquet, M.; Touchard, D.; Bruneau, C.; Dixneuf, P. H. *New J. Chem.* **1999**, 141–143.

(6) Castarlenas, R.; Dixneuf, P. H. *Angew. Chem., Int. Ed.* **2003**, *42*, 4524–4527.

(7) Bassetti, M.; Centola, F.; Sémeril, D.; Bruneau, C.; Dixneuf, P. H. *Organometallics* **2003**, *22*, 4459–4486.

(8) (a) Jafarpour, L.; Schanz, H.-J.; Stevens, E. D.; Nolan, S. P. *Organometallics* **1999**, *18*, 5416–5419. (b) Fürstner, A.; Thiel, O. R.; Ackermann, L.; Schanz, H.-J.; Nolan, S. P. *J. Org. Chem.* **2000**, *65*, 2204–2207. (c) Fürstner, A.; Guth, O.; Düffels, A.; Seidel, G.; Liebl, M.; Gabor, B.; Mynott, R. *Chem.—Eur. J.* **2001**, *7*, 4811–4820. (d) Opstal, T.; Verpoort, F. *Angew. Chem., Int. Ed.* **2003**, *42*, 2876–2879. (e) Clavier, H.; Nolan, S. P. *Chem.—Eur. J.* **2007**, *13*, 8029–8036. (f) Stijn, M.; Drozdak, R.; Dragutan, V.; Dragutan, I.; Verpoort, F. *Eur. J. Inorg. Chem.* **2008**, 432–440.

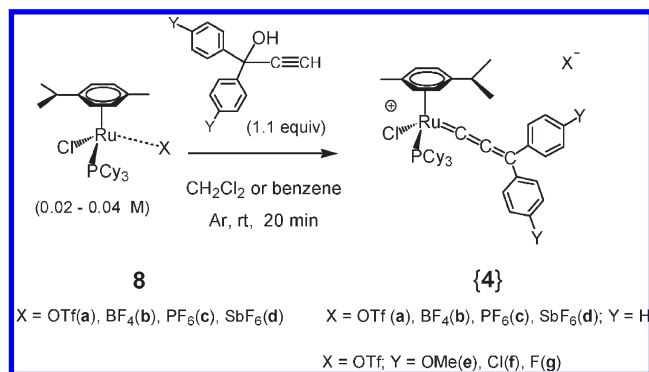
(9) Schanz, H.-J.; Jafarpour, L.; Stevens, E. D.; Nolan, S. P. *Organometallics* **1999**, *18*, 5187–5190.

(10) The complexes were obtained from the reaction of $[\text{RuCl}_2(p\text{-cymene})_2]$ or $[\text{Ru}(\text{Cl}_2)(\text{PPh}_3)_4]$ with 3,3-diphenylpropyn-3-ol in the presence of PCy_3 and subsequent phosphine exchange for the N-heterocyclic carbene ligand. The same reaction in the absence of excess phosphine afforded the corresponding 3-phenyl-1-indenylidene complexes, as active RCM catalyst (ref 8a).

(11) Reviews: (a) Dragutan, V.; Dragutan, I.; Verpoort, F. *Platinum Met. Rev.* **2005**, *49*, 33–40. (b) Boeda, F.; Clavier, H.; Nolan, S. P. *Chem. Commun.* **2008**, 2726–2740. (c) Clavier, H.; Correa, A.; Escudero-Adan, E. C.; Benet-Buchholdz, J.; Cavallo, L.; Nolan, S. P. *Chem.—Eur. J.* **2009**, *15*, 10244–10254. (d) Lozano-Vila, A. M.; Monsaert, S.; Bajek, A.; Verpoort, F. *Chem. Rev.* **2010**, *110*, 4865–4909.

(12) Castarlenas, R.; Vovard, C.; Fischmeister, C.; Dixneuf, P. H. *J. Am. Chem. Soc.* **2006**, *128*, 4079–4089.

(13) Shaffer, E. A.; Chen, C. L.; Beatty, A. M.; Valente, E. J.; Schanz, H. J. *J. Organomet. Chem.* **2007**, *692*, 5221–5233.

Scheme 2. Preparation of the Allenylidene Complexes To Be Used *in Situ* for ^1H NMR or UV–Vis Measurements


indenylidene rearrangement in complexes with varying counteranions and aryl substituents, in the absence of olefin, thus providing a convergent mechanistic picture about the initiation stage of the cationic ruthenium(II) allenylidene complexes in alkene metathesis.

Results and Discussion

Our previous kinetic investigation regarded the RCM reaction of the 1,6-diene **7** into *N*-tosyl-2,5-dihydropyrrole, catalyzed by the allenylidene complexes $[(\eta^6\text{-}p\text{-cymene})\text{RuCl}(\text{=C=C=C}\text{Ar}_2)\text{PR}_3][\text{X}]$ (Ar = Ph, X = OTf (**4a**), BF₄[−] (**4b**), PF₆[−] (**4c**), and SbF₆[−] (**4d**); X = OTf, Ar = *p*-MeOC₆H₄ (**4e**), Ar = *p*-ClC₆H₄ (**4f**), and Ar = *p*-FC₆H₄ (**4g**)). The complexes, synthesized from the reaction of the cationic precursors $[(\eta^6\text{-}p\text{-cymene})\text{RuCl}(\text{PCy}_3)][\text{X}]$ (X = OTf (**8a**), BF₄[−] (**8b**), PF₆[−] (**8c**), SbF₆[−] (**8d**)) with the propargylic alcohols (4-YC₆H₄)₂C(OH)C≡CH (Y = H, OMe, Cl, F), were isolated and used afterward in the catalytic tests.⁷ In this work, the allenylidene complexes were prepared from the same precursors but used directly *in situ* (**4a**), thus avoiding the separation and purification procedures, as well as possible aging (Scheme 2). The formation of the desired allenylidene complex was confirmed by ³¹P NMR. As examples, the ³¹P NMR spectra of the solution of complex **8a** in benzene-*d*₆, or complex **8d** in dichloromethane-*d*₂, with Ph₂C(OH)C≡CH (1.1 molar equiv), recorded 20 min after addition of the solvent into the NMR tube, showed nearly quantitative conversion of the ruthenium precursor into the corresponding allenylidene complex, other species not being detected (see Figures 1 and 2 in the Supporting Information). Thus, the mechanistic information regarding the thermally induced allenylidene–indenylidene rearrangement was obtained (i) from the kinetics of RCM of *N,N*-diallyltosylamide **7** in the presence of complex **4a**, by ¹H NMR spectroscopy, and (ii) from kinetic measurements of the spontaneous transformation in solution of the allenylidene complexes **4a–g** by UV–visible spectroscopy.

Kinetics of RCM of *N,N*-Diallyltosylamide. The study performed on the series of isolated allenylidene complexes **4a–g** showed that the conversion of **7** into *N*-tosyl-2,5-dihydropyrrole proceeded in the presence of the allenylidene complex **4a** with the highest reactivity and selectivity (>90%) with respect to the complexes with different counteranions or with aryl *para*-substituents and was faster in benzene-*d*₆ than in dichloromethane-*d*₂. The nature of the solvent (C₆D₆ or CD₂-Cl₂) led to very different kinetic data. The zero-order dependence on olefin in dichloromethane-*d*₂ suggested rate-determining transformation of the allenylidene complex into the catalytically active species, followed by faster RCM.⁷ In this work,

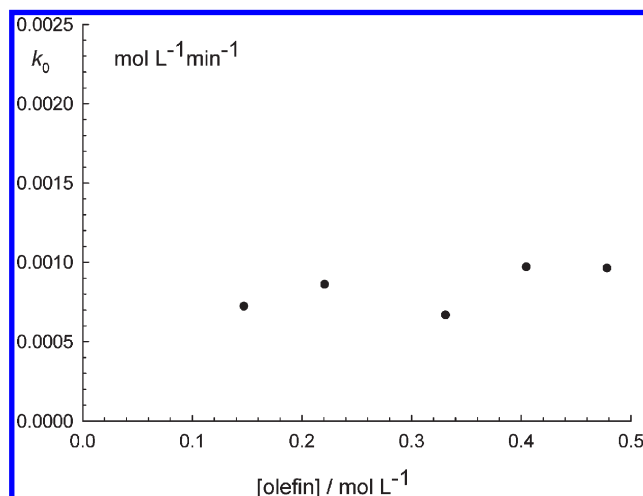
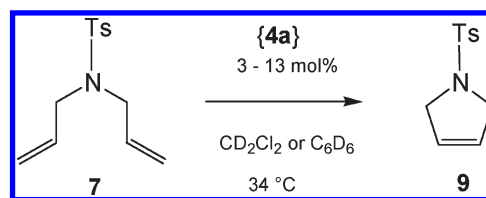


Figure 1. Zero-order rate constants (k_0) for the reaction of diallyltosylamide (**7**) catalyzed by complex $[(\eta^6\text{-}p\text{-cymene})\text{RuCl}(\text{=C=C=C}\text{Ph}_2)\text{PCy}_3][\text{OTf}]$ (**4a**) (0.026 ± 0.001 M), as a function of the initial olefin concentration, in dichloromethane-*d*₂ (33.9 °C).

Scheme 3. RCM Reaction of *N,N*-Diallyltosylamide, Catalyzed by $[(\eta^6\text{-}p\text{-cymene})\text{RuCl}(\text{=C=C=C}\text{Ph}_2)\text{PCy}_3][\text{OTf}]$ Formed *in Situ*


the RCM rates were measured at varying concentrations of both olefin and catalyst **4a** in benzene-*d*₆ or in dichloromethane-*d*₂, under the conditions outlined in Scheme 3. The samples were obtained upon addition of the olefin to solutions of weighted amounts of complex $[\text{Ru}(\eta^6\text{-}p\text{-cymene})\text{Cl}(\text{PCy}_3)]$ (**8a**) and Ph₂C(OH)C≡CH in the NMR tube, and the reaction progress was then monitored by ¹H NMR spectroscopy. The zero-order rate constants of the reactions in dichloromethane-*d*₂, as determined from the slope in the linear plots of **7** vs time, increased linearly with the concentration of the catalyst precursors in the range 0.074–0.0437 mol L^{−1} (**7**) = 0.331 mol L^{−1}), indicating first-order rate dependence on the ruthenium complex. Conversely, the rate constants were virtually independent of olefin concentration in the range **7** = 0.147–0.478 M, with an average value of $k_0 = 1.4 \times 10^{-5}$ mol L^{−1} s^{−1} at 33.9 °C (Figure 1).

These measurements are in agreement with the value $k_0 = 1.1 \times 10^{-5}$ mol L^{−1} s^{−1} (33.0 °C) obtained for the reaction of **7** performed in the presence of an isolated sample of complex **4a**.⁷ This kinetic behavior implies that the rate of metathesis is not affected by the initial olefin concentration within the range commonly used to perform RCM reactions.

The reactions in benzene-*d*₆ catalyzed by **4a** exhibited a complex kinetic behavior. The reactions proceeded quantitatively at low olefin/complex molar ratios, and the rate data were fitted properly by the first-order rate equation. Under the conditions **7** = 0.087 M and **4a** = 0.015 M at 34.7 °C, the exponential fitting of the experimental data gave a value of observed rate constant $k_{\text{obs}} = 1.68 \times 10^{-4}$ s^{−1}, indicating first-order rate dependence on the olefin and hence rate-limiting RCM. However, measurements at higher concentration of diene showed a linear

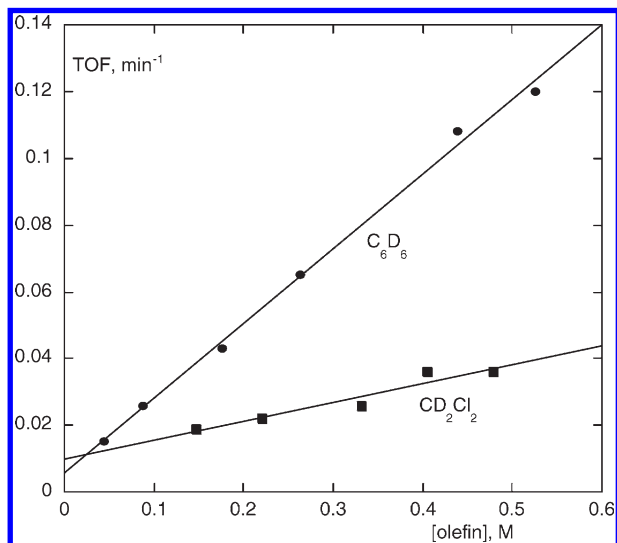


Figure 2. Plot of TOF values vs initial concentration of *N,N*-diallyltosylamide (**7**), for the reactions catalyzed by complex $[(\eta^6\text{-}p\text{-cymene})\text{RuCl}(\text{C}=\text{C}=\text{CPh}_2)\text{PCy}_3][\text{OTf}]$ (**4a**) in benzene- d_6 ($[\mathbf{4a}] = 0.0131\text{--}0.0154\text{ M}$) and in dichloromethane- d_2 ($[\mathbf{4a}] = 0.0252\text{--}0.0283\text{ M}$), at $34.5\text{ }^\circ\text{C}$.

decrease of substrate concentration, according to zero-order rate dependence, and incomplete conversions, as the result of catalyst decomposition at the extended reaction times required for consumption of higher olefin loads. To facilitate the analysis of the reactivity in the two solvents and at varying diene concentrations, the turnover frequency values (TOF, min^{-1}), which reflect the slowest step in the overall catalytic process (initiation and propagation), were taken into account.¹⁴ The plots of the TOF values vs the initial concentration of olefin (Figure 2) display a higher reactivity in benzene- d_6 than in dichloromethane- d_2 , in spite of the larger precatalyst load that was necessary in the latter solvent in order to observe significant conversions into product. The efficiency of the catalytic system in the aromatic solvent is also indicated by the steady increase of conversion with increasing olefin load, without showing product inhibition up to a olefin concentration of 0.5 M.

This set of experimental data is consistent with the occurrence of a molecular transformation of the allenylidene complex that precedes the catalytic cycle of the RCM reaction. In dichloromethane, this process is slower than RCM, thus being rate limiting and producing a ring-closure reaction that is zero-order in olefin. The same process is favored in benzene- d_6 , showing a 2–3-fold increase of the k_0 rate constant or first-order dependence on the diene at low $[\mathbf{7}]$.

The RCM of the diene **7** was monitored in the presence of acid. When HBF_4 (0.075 mmol, $[\text{H}^+]/[\text{Ru}] = 5$) and then the olefin (0.197 mmol, 0.32 M, $[\mathbf{7}]/[\text{Ru}] = 13$) were added to a solution of complex **8a** (0.015 mmol) and $\text{Ph}_2\text{C}(\text{OH})\text{C}\equiv\text{CH}$ in dichloromethane- d_2 (0.55 mL), substrate consumption and product formation were complete after about 10 min of reaction, at rt. This observation, consistent with the expected rate

(14) $\text{TOF} = (\text{moles of } \mathbf{7} \times \% \text{ conversion of } \mathbf{7}) / (\text{moles of } \{\mathbf{4a}\} \times \text{time})$. These were measured at the same reaction time in all runs (200 min), when the conversion of the olefin was in the range 44–67% in dichloromethane- d_2 , and in the range 68–98% in benzene- d_6 (see the table of experimental data in the SI).

(15) The same diene was converted into **9** with 99% yield in the presence of complex **4a** and a 5-fold excess of TfOH , in 30 min at $0\text{ }^\circ\text{C}$ (ref 6).

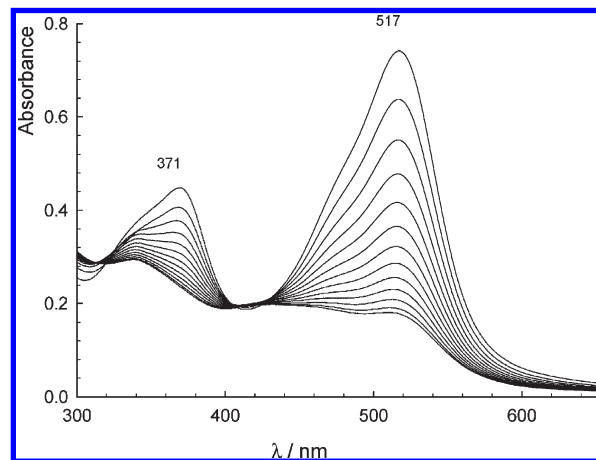


Figure 3. Sequence of UV–visible spectra of complex $[(\eta^6\text{-}p\text{-cymene})\text{RuCl}(\text{C}=\text{C}=\text{CPh}_2)\text{PCy}_3][\text{OTf}]$ (**4a**), in dichloromethane ($38\text{ }^\circ\text{C}$, cycle time 40 min).

enhancement produced by the presence of a strong proton donor,¹⁵ further validates the effectiveness of the procedure for the formation and use *in situ* of the allenylidene complex **4a**, which is rapidly transformed into the active indenylidene derivative upon acid addition (Scheme 1, route a).

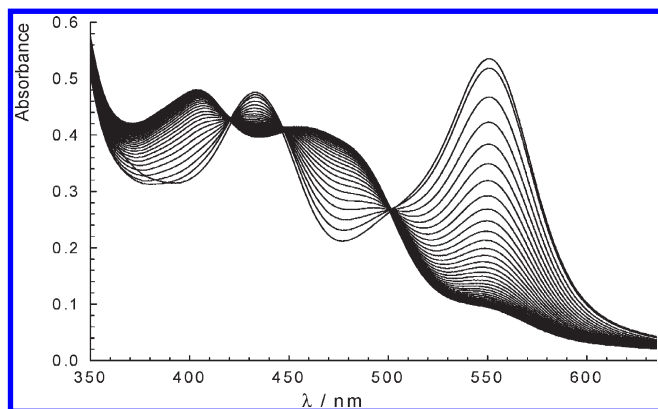
Solution Reactivity of the Allenylidene Complexes. When a solution of complex **4a** in toluene was heated at $50\text{ }^\circ\text{C}$, the spectroscopic absorptions of the allenylidene moiety, i.e., the infrared (1970 cm^{-1}) and the UV–visible (518 nm) bands, were observed to disappear in about 15 min, thus indicating in particular a transformation of the unsaturated group.⁷ Such a transformation has been studied here in detail by UV–visible spectroscopy. The stock solutions of complexes **8** and the propargylic alcohols, in dichloromethane or in benzene, were diluted in order to obtain suitable concentration values ($10^{-4}\text{--}10^{-5}\text{ M}$) of the ruthenium complex. A sequence of UV–visible spectra obtained upon warming the dichloromethane solution of the resulting complex **4a** is shown in Figure 3 ($38\text{ }^\circ\text{C}$). Fitting the disappearance of the 517 nm band with the first-order rate equation gave the value of the observed rate constant, $k_{\text{obs}} = 6.4 \times 10^{-5}\text{ s}^{-1}$, corresponding to a half-life ($\tau_{1/2}$) of 180 min. In benzene, the same complex underwent a more involved and rapid transformation even at room temperature. The first-order fitting of the absorption changes at 517 nm yielded a value of $k_{\text{obs}} = 2.9 \times 10^{-4}\text{ s}^{-1}$, corresponding to $\tau_{1/2} = 40\text{ min}$ ($25\text{ }^\circ\text{C}$).¹⁶ Still in benzene, the bis(*p*-methoxybenzene)allenylidene complex **4e** ($\text{X} = \text{OTf}$, $\text{Ar} = p\text{-MeOC}_6\text{H}_4\text{-}$) exhibited a slower transformation ($\tau_{1/2} = 167\text{ min}$, $25\text{ }^\circ\text{C}$) and afforded a relatively stable species with respect to its phenyl analogue, as indicated by the presence of isosbestic points in the sequence of UV–visible spectra (Figure 4).

The k_{obs} values obtained from the decay of the UV–visible allenylidene band of complexes **4a–g** are reported in Table 1. The reactions are faster in benzene than in dichloromethane for all compounds, to the extent that the *p*-methoxyallenylidene complex did not react in dichloromethane even near the boiling temperature ($38\text{ }^\circ\text{C}$). When it is possible to obtain k_{obs} values at $25\text{ }^\circ\text{C}$ in both solvents, the ratio $k_{\text{benzene}}/k_{\text{DCM}}$ changes from 2.2 for the PF_6 complex **4c** to 6.6 for the triflate analogue.

(16) At $35\text{ }^\circ\text{C}$, the value $k_{\text{obs}} = 6.8 \times 10^{-4}\text{ s}^{-1}$ of the allenylidene disappearance agrees well with the observed first-order consumption of the olefin **7** in the RCM process at the same temperature ($k_1 = 1.7 \times 10^{-4}\text{ s}^{-1}$) and the proposal of faster activation stage than olefin metathesis under these conditions in benzene- d_6 .

Table 1. Values of k_{obs} (s^{-1}) for the Decay of the Allenylidene Band of Complexes {4a–g}, in Benzene and in Dichloromethane

entry	complex	Ar/X	T ($^{\circ}\text{C}$)	k_{obs} , s^{-1} in CH_2Cl_2	k_{obs} , s^{-1} in C_6H_6
1	{4a}	Ph/OTf	50		3.7×10^{-3}
			43		1.8×10^{-3}
			38	6.4×10^{-5}	
			35		6.8×10^{-4}
			25	4.4×10^{-5}	
			18		2.9×10^{-4}
2	{4b}	Ph/BF ₄ [−]	38	6.0×10^{-5}	
			25		3.9×10^{-4}
3	{4c}	Ph/PF ₆ [−]	38	4.9×10^{-5}	
			25	1.2×10^{-5}	2.6×10^{-5}
4	{4d}	Ph/SbF ₆ [−]	38	5.1×10^{-5}	
			25		2.2×10^{-5}
			25		2.7×10^{-3}
5	{4e}	<i>p</i> -MeOC ₆ H ₄ /OTf	55		8.7×10^{-4}
			45		
			38	too slow	
			35		2.5×10^{-4}
			25		6.9×10^{-5}
6	{4f}	<i>p</i> -ClC ₆ H ₄ /OTf	38	1.0×10^{-4}	
			25		4.0×10^{-4}
			25		4.0×10^{-4}
7	{4g}	<i>p</i> -FC ₆ H ₄ /OTf	38	7.1×10^{-5}	
			25		5.4×10^{-4}

**Figure 4.** Sequence of UV–visible spectra of complex $[(\eta^6\text{-}p\text{-cymene})\text{RuCl}\{\text{=C=C=C}(p\text{-MeOC}_6\text{H}_4)_2\}\text{PCy}_3][\text{OTf}]$, in benzene ($25\text{ }^{\circ}\text{C}$, cycle time 30 min).

Within the series of phenyl allenylidene complexes {4a–d}, there is a negligible effect of the counteranions in dichloromethane at $38\text{ }^{\circ}\text{C}$, whereas at $25\text{ }^{\circ}\text{C}$ the triflate complex is more reactive than the corresponding hexafluorophosphate species by a factor of 3.6. The reactivity of the same pair of complexes differs by a factor of 11 in benzene at $25\text{ }^{\circ}\text{C}$, thus indicating a larger counteranion effect in the latter solvent. The fact that the *p*-methoxybenzene derivative {4e} ($\text{X} = \text{OTf}$) undergoes transformation even at $25\text{ }^{\circ}\text{C}$ further indicates the relevance of the counteranion contact in benzene. These decay k_{obs} values allow establishing the sequence of influence of the interaction of the counteranions for the salt in benzene: $\text{BF}_4^- > \text{OTf} \gg \text{PF}_6^- > \text{SbF}_6^-$.

Measurements in benzene at different temperatures and the corresponding Eyring plots gave the values of the activation

parameters of complexes $[(\eta^6\text{-}p\text{-cymene})\text{RuCl}\{\text{=C=C=C}(\text{Ph})_2\}\text{PCy}_3][\text{OTf}]$ ($18\text{--}50\text{ }^{\circ}\text{C}$) and $[(\eta^6\text{-}p\text{-cymene})\text{RuCl}\{\text{=C=C=C}(p\text{-MeOC}_6\text{H}_4)_2\}\text{PCy}_3][\text{OTf}]$ ({4e}, $25\text{--}55\text{ }^{\circ}\text{C}$), which are $\Delta H^\ddagger = 22 \pm 2\text{ kcal mol}^{-1}$ and $\Delta S^\ddagger = -1 \pm 5\text{ cal mol}^{-1}\text{ K}^{-1}$, and $\Delta H^\ddagger = 24 \pm 1\text{ kcal mol}^{-1}$ and $\Delta S^\ddagger = 1 \pm 1\text{ cal mol}^{-1}\text{ K}^{-1}$, respectively.

The UV–visible spectra of complex 4a were also monitored in the presence of HBF_4 , in dichloromethane. The addition of the acid resulted in rapid decay of the allenylidene band, in agreement with its initial transformation into an alkenylcarbyne fragment, as intermediate species toward the corresponding indenylidene derivative (Scheme 1, route a).¹⁷ The derived first-order rate constants, k_{obs} , increased linearly with the concentration of the acid, as shown in the plot of Figure 5. The slope of the linear fitting corresponds to the second-order rate constant for the reaction of complex {4a} with HBF_4 , being $k_2 = 0.050\text{ M}^{-1}\text{ s}^{-1}$. In addition, the $k_{\text{obs}}/[\text{HBF}_4]$ plot exhibits a positive intercept on the y axis, which highlights the presence of a reaction pathway independent of the acid.

The kinetic analysis indicates that the disappearance of the allenylidene band proceeds via parallel pathways, one being first-order in ruthenium complex and first-order in acid (overall second-order) and one being first order in the ruthenium complex and zero-order in acid (overall first-order).¹⁸ This is represented graphically in the plot, and it

(17) The reaction of complex 4a with triflic acid was studied in detail by low-temperature NMR spectroscopy in dichloromethane-*d*₂, which allowed the observation of the alkenylcarbyne intermediate at $-40\text{ }^{\circ}\text{C}$ and of the derived indenylidene complex at $-20\text{ }^{\circ}\text{C}$. These species were extensively characterized by ^1H , $^{31}\text{P}\{^1\text{H}\}$, and $^{13}\text{C}\{^1\text{H}\}$ NMR, including $^1\text{H}\text{--}^{13}\text{C}$ HMQC experiments (refs 6 and 12).

(18) (a) Maskill, H. *The Physical Basis of Organic Chemistry*; Oxford University Press: New York, 1985; pp 276–278. (b) Atwood, J. D. *Inorganic and Organometallic Reaction Mechanisms*; Brooks/Cole Publishing Company: Monterey, CA, 1985; pp 12–14.

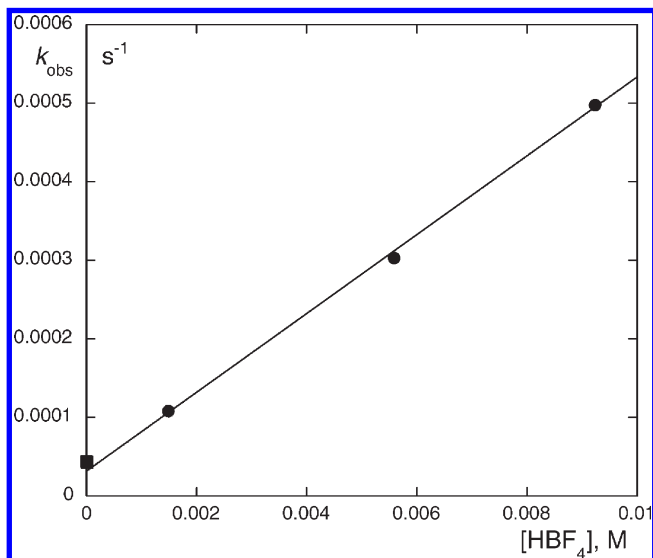


Figure 5. Plot of k_{obs} values for the rearrangement of complex $[(\eta^6\text{-}p\text{-cymene})\text{RuCl}\{\text{C}=\text{C}=\text{C}(\text{Ph})_2\}\text{PCy}_3][\text{OTf}]$, prepared *in situ*, in the presence (●) or absence (■) of HBF_4 (dichloromethane, 25 °C).

is described by the rate equations 1 and 2.

$$-\text{d}[\{\mathbf{4a}\}]/\text{d}t = k_1[\{\mathbf{4a}\}] + k_2[\{\mathbf{4a}\}][\text{HBF}_4] \quad (1)$$

$$k_{\text{obs}} = -\text{d}[\{\mathbf{4a}\}]/\text{d}t \times 1/[\{\mathbf{4a}\}] = k_1 + k_2[\text{HBF}_4] \quad (2)$$

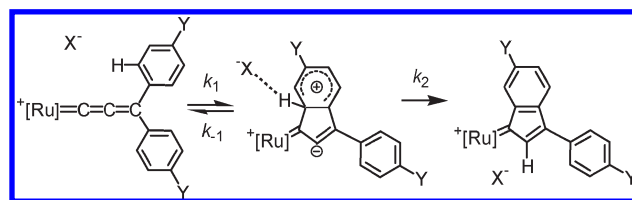
The second-order pathway, expressed by the linear dependence of k_{obs} on $[\text{HBF}_4]$, corresponds to rate-determining proton attack on the unsaturated moiety, while the first-order pathway, expressed by the y intercept, corresponds to the spontaneous, acid-free transformation. Furthermore, the intercept value ($3.2 \times 10^{-5} \text{ s}^{-1}$) agrees well with the rate constant of the thermally induced rearrangement of $\{\mathbf{4a}\}$ at 25 °C measured in the absence of acid (Table 1, entry 1). Therefore, under these conditions, the allenylidene–indenylidene transformation proceeds via parallel acid-induced and thermally induced pathways, the contribution of the latter being large at low $[\text{HBF}_4]$, while becoming increasingly smaller with increasing acid concentration.

At this point, it appears informative to compare the results of the kinetics of the RCM catalytic process and of the unimolecular transformation of the allenylidene complexes, which display parallel solvent, counteranion, proton, and aryl substituent effects. In particular, both processes proceed at faster rates in benzene than in dichloromethane. While the allenylidene absorption of the triflate derivative $\{\mathbf{4a}\}$ decays 1 order of magnitude more rapidly than in the corresponding PF_6^- and SbF_6^- salts (in benzene), the preformed complex $\mathbf{4a}$ was found to be the most active precatalyst in RCM and polymerization reactions.¹⁹ The allenylidene complex $\mathbf{4e}$ ($\text{Ar} = p\text{-MeOC}_6\text{H}_4-$, $\text{X} = \text{OTf}$), bearing the p -methoxy substituent in the benzene rings, did not promote efficient olefin metathesis of diene **7** and showed a significant induction time period, suggesting slow conversion of the precatalyst into the catalytically active species.^{7,20} In agreement

(19) Specific effects of the escorting counterions on the olefin metathesis activity were previously described and discussed in detail in refs 3b and 4b.

(20) Ligand electronic substituent effects on ruthenium-catalyzed RCM rates have been studied in Ru(II) catecholate catalysts: Monfette, S.; Camm, K. D.; Gorelsky, S. I.; Fogg, D. E. *Organometallics* **2009**, *28*, 944–946.

Scheme 4. Proposed Mechanism of the Ruthenium Allenylidene–Indenylidene Rearrangement ($[\text{Ru}] = [\text{Ru}(\eta^6\text{-}p\text{-cymene})\text{CIPCy}_3]$)



with the metathesis activity, complex $\{\mathbf{4e}\}$ is the most stable in both solvents with respect to the $p\text{-Cl}$, $p\text{-F}$, and phenyl analogues. These can be regarded as evidence that the allenylidene group rearranges into the corresponding indenylidene, as active species of the olefin metathesis process.

Mechanism of the Thermally Induced Allenylidene–Indenylidene Rearrangement. The mechanism of the acid-free transformation of the allenylidene complexes can be described in terms of an intramolecular electrophilic aromatic substitution,²¹ according to the known electrophilic character of the allenylidene α -carbon atom of ruthenium complexes.²² A mechanistic view of the process is shown in Scheme 4. It is composed of a two-stage sequence involving (i) a reversible C–C bond forming step, in which the electrophilic C_α is attacked by the *ortho*-carbon of the phenyl ring, and (ii) an irreversible proton migration from the benzene to the β -carbon atom across the newly formed five-membered ring. The transformation implies the formation of an arenium ion intermediate (k_1), which competes between C–C bond breaking to generate the starting material (k_{-1}) or H-shift to form the indenylidene fragment (k_2). In the present case, the arenium ion intermediate forms with charge separation, since the electrophilic species is the dipole $\text{Ru}=\text{C}_\alpha^{(\delta+)}=\text{C}_\beta^{(\delta-)}$.

The kinetic analysis of the proposed mechanism with application of the steady-state approximation to the transient arenium ion intermediate affords the rate equation 3. The partitioning of the σ complex back to the allenylidene or forward to indenylidene depends on the ease with which the C_α electrophile is released relative to the proton.

$$k_{\text{obs}} = k_1 k_2 / (k_{-1} + k_2) \quad (3)$$

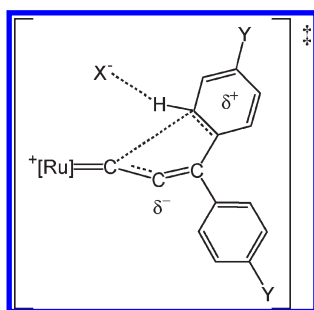
The Eyring plots obtained for the transformation of the triflate allenylidene complexes $\{\mathbf{4a}\}$ ($\text{Y} = \text{H}$) and $\{\mathbf{4e}\}$ ($\text{Y} = \text{OMe}$) in benzene gave the same values, within experimental error, of entropy of activation, indicating that the aryl substituent does not influence the geometry of the transition state. The difference in reactivity arises essentially from the substituent electronic effects affecting the ΔH^\ddagger parameter and hence from the energy changes involved in the C–C bond forming step. Moreover, the ΔS^\ddagger values near zero suggest that the entropy of the reactant is similar to that of the activated complex, which therefore forms with little skeletal rearrangement.²³ The occurrence of a rate-determining dissociative process such as a phosphine-releasing step, which would imply positive ΔS^\ddagger values, can therefore be

(21) Smith, M. B.; March, J. In *March's Advanced Organic Chemistry*; John Wiley & Sons: NJ, 2007; Chapter 11.

(22) (a) Bruce, M. I. *Chem. Rev.* **1998**, *98*, 2797–2858. (b) Cadierno, V.; Gimeno, J. *Chem. Rev.* **2009**, *109*, 3512–3560.

(23) (a) Anslyn, E. V.; Dougherty, D. A. In *Modern Physical Organic Chemistry*; University Science Books: Sausalito, CA, 2006, p 412. The values of entropies of activation are consistent with the occurrence of an intramolecular ring-closing process forming a five-membered ring: (b) Galli, C.; Mandolini, L. *Eur. J. Org. Chem.* **2000**, 3117–3125. (c) Illuminati, G.; Mandolini, L. *Acc. Chem. Res.* **1981**, *14*, 95–102.

Chart 2



excluded.²⁴ On the other hand, phosphine release occurs in the initiation and propagation stages of the first- and second-generation Grubbs catalysts **1** and **2**, and it is rate determining for phosphine exchange, with entropies of activation of 12 and 13 eu, respectively, and for olefin substitution, in agreement with operative dissociative mechanisms.²⁵

Regarding the aryl substituent effects in the series of the *para*-substituted allenylidenes, the data reported in Table 1 reveal small rate changes between the phenyl and the *p*-Cl or *p*-F derivatives (entries 1, 6, 7). Such modest rate changes suggest an early transition state in the first step, i.e., reactant-like, with modest σ bond formation and little C–H bond breaking (Chart 2). The incurring charge separation that occurs within the organic fragment in the transition state toward the intermediate arenium ion can also account for resulting counterbalanced effects of the aryl substituents Y. On the other hand, the *p*-MeO groups exhibit a distinct deactivating effect, which varies from a factor of 8 (k_F/k_{OMe}) in benzene to one exceedingly large in dichloromethane, in which the allenylidene moiety of **4e** does not rearrange. This is still consistent with a reactant-like transition state in step 1, in which the electron-donating influence of *p*-methoxy by resonance (+*R*) makes the allenylidene less electrophilic in the ground state and destabilizes the developing negative charge on C $_{\beta}$ in the forming arenium ion. Moreover, since the attacking ring carbon is *meta* with respect to the MeO substituent, it is reasonable to assume that the dominant electron-withdrawing field effect (–*I*) of the methoxy group reduces the carbon nucleophilic character and deactivates the reaction.

By contrast, classic bimolecular electrophilic aromatic substitutions, characterized by rate-determining electrophile–C(sp²) bond formation and rapid H uptake by base, are accelerated by electron-donating ring substituents and exhibit large and negative ρ values in linear free energy relationships, with substituent electronic effects varying over orders of

(24) This point was difficult to ascertain via the classic approach of performing kinetic runs in the presence of free phosphine, which would retard the reaction rate. In fact, the addition of excess PCy₃ to solutions of the allenylidene complexes caused rapid decomposition, as observed by the immediate change of color from deep red to yellow. On the basis of the observed activation entropies, it is reasonable to assume that such a step is not involved, or is not rate determining, in the transformation of the allenylidene complexes. Nevertheless, a strong correlation with the nature of the bound phosphine in the allenylidene catalysts was observed in the RCM of **7**, which decreased in the order PCy₃ > PiPr₃ >> PPh₃ (ref 3a), whereas the presence of free PCy₃ changed the reaction course from ring-closing to allylic isomerization (ref 7).

(25) (a) Sanford, M. S.; Uman, M.; Grubbs, R. H. *J. Am. Chem. Soc.* **2001**, *123*, 749–750. (b) Sanford, M. S.; Love, J. A.; Grubbs, R. H. *J. Am. Chem. Soc.* **2001**, *123*, 6543–6554.

(26) (a) Stock, L. M.; Brown, H. C. *Adv. Phys. Org. Chem.* **1963**, *1*, 35–154. (b) Rys, P.; Skrabal, P.; Zollinger, H. *Angew. Chem., Int. Ed. Engl.* **1972**, *11*, 874–883.

magnitude of reactivity.^{18a,26} The direction and the extent of the electronic effect are related to the transition-state geometry, resembling that of the arenium ion intermediate, with fully developed positive charge.

Although an anion-dependent switch in reaction selectivity has been demonstrated for the C–H activation of imidazolium salts by an iridium complex,²⁷ the influence of the counteranions X on the rearrangement of these ruthenium complexes is not obvious. In particular, the highest activity exhibited by the triflate and tetrafluoroborate complexes in benzene, with respect to the PF₆[–] and SbF₆[–] complex analogues, needs to be discussed. It can be argued that the smallest and coordinating anions, characterized by highest charge density, facilitate charge dissipation in the σ complex, via generic cation–anion interactions or even via specific hydrogen bonding with the proton of the benzene ring. The counteranion in close contact with the ruthenium cation can assist C–H bond breaking and facilitate the proton migration from the benzene ring to the C $_{\beta}$ carbon by acting as proton shuttle between the two carbon atoms. The action of a proton shuttle would increase the ratio $k_2/(k_{-1} + k_2)$ in the competition of the arenium ion for C–C bond breaking (k_{-1}) or H migration (k_2). Various examples of organometallic reaction mechanisms based on counteranion proton shuttles have been documented in the literature.^{27,28} These hypotheses find substantial support in the distinct rate differences observed in benzene and in dichloromethane. In fact, the preference of organometallic salts for contact ion pairs in benzene, and hence for direct cation–anion interactions, and for solvent-separated ion pairs in more polar solvents is well documented.²⁹ The latter situation accounts for the observed flattening of counteranion effects in dichloromethane. Specifically, higher levels of aggregation in benzene vs dichloromethane have been determined by diffusion and NOE NMR experiments in the case of cationic *p*-cymene ruthenium(II) complexes.³⁰ It is worth mentioning that the electrophilic activation of H–C(sp²) bonds by intermolecular or intramolecular interactions with coordinated ligands, in particular oxygenated anions, is gaining increasing recognition and interest in organometallic catalysis.^{31,32}

Conclusion

The allenylidene to indenylidene rearrangement proceeds at a faster rate in benzene than in dichloromethane, and this

(27) Appelhans, L. N.; Zuccaccia, D.; Kovacevic, A.; Chianese, A. R.; Miecznikowski, J. R.; Macchioni, A.; Clot, E.; Eisenstein, O.; Crabtree, R. H. *J. Am. Chem. Soc.* **2005**, *127*, 16299–16311.

(28) (a) Zang, G.; Shen, W.; Li, L.; Li, M. *Organometallics* **2009**, *28*, 3129–3139. (b) Kovacs, G.; Ujaque, G.; Lledos, A. *J. Am. Chem. Soc.* **2008**, *130*, 853–864. (c) Shi, F.-Q.; Li, X.; Xia, Y.; Zhang, L.; Yu, Z.-X. *J. Am. Chem. Soc.* **2007**, *129*, 15503–15512. (d) Lafrance, M.; Fagnou, K. *J. Am. Chem. Soc.* **2006**, *128*, 16496–16497. (e) Quadrelli, E. A.; Kraatz, H.-B.; Poli, R. *Inorg. Chem.* **1996**, *35*, 5154–5162.

(29) Macchioni, A. *Chem. Rev.* **2005**, *105*, 2039–2073.

(30) Zuccaccia, D.; Bellachioma, G.; Cardaci, G.; Ciancaleoni, G.; Zuccaccia, C.; Clot, E.; Macchioni, A. *Organometallics* **2007**, *26*, 3930–3946.

(31) (a) García-Cuadrado, D.; de Mendoza, P.; Braga, A. A. C.; Maseras, F.; Echavarren, A. M. *J. Am. Chem. Soc.* **2007**, *129*, 6880–6886. (b) Özdemir, I.; Demir, S.; Çetinkaya, B.; Gourlaouen, C.; Maseras, F.; Bruneau, C.; Dixneuf, P. H. *J. Am. Chem. Soc.* **2008**, *130*, 1156–1157. (c) Požgan, F.; Dixneuf, P. H. *Adv. Synth. Catal.* **2009**, *351*, 1737–1743.

(32) The concept of bifunctional organometallic catalysis resulting from ligands capable of proton transfer or hydrogen bonding has been recently reviewed: Grotjahn, D. B. *Pure Appl. Chem.* **2010**, *82*, 635–647.

is explained by a stronger interaction of the counteranion with the cationic rearranging species in the less polar aromatic solvent. The first-order rate constants, k_{obs} , for the phenyl complexes depend on the counteranion nature and decrease in the order $\text{BF}_4^- > \text{CF}_3\text{SO}_3^- \gg \text{PF}_6^- > \text{SbF}_6^-$, in benzene. The allenylidene complex **4e**, with donating *p*-methoxy groups, is the most stable among the series of *para*-substituted derivatives and does not lead to indenylidene in dichloromethane. The RCM reaction of diallyltosylamide and the spontaneous or thermally induced transformation of the *p*-cymene allenylidene ruthenium complexes are characterized by parallel solvent, proton, counteranion, and aryl substituent effects, thus providing evidence that the catalytic reaction requires the rearrangement of the allenylidene group into the corresponding indenylidene, as active species of the acid-free olefin metathesis process. The recognition of the solvent and of the counteranion effects in terms of the operative mechanism of the allenylidene–indenylidene rearrangement may provide novel clues for the design of more effective metathesis catalysts. For instance, the presence in the propargylic alcohol of aromatic rings with increased reactivity toward electrophilic aromatic substitution may cause faster allenylidene rearrangement and thus direct access to the active indenylidene complexes starting from the easily accessible cationic precursors $[(\eta^6\text{-}p\text{-cymene})\text{RuCl}(\text{PCy}_3)][\text{X}]$.

Experimental Section

General Procedures. The manipulations were performed under an atmosphere of dry argon using vacuum-line and standard Schlenk techniques. Dichloromethane was distilled over CaH_2 and benzene over Na/K alloy, under argon. ^1H and ^{31}P NMR spectra were obtained on a Bruker AC 300 P spectrometer, operating at 300.13 and 121.5 MHz, respectively. ^1H chemical shifts are referenced to δ 7.26 (CHCl_3) or 5.35 (CH_2Cl_2) ppm, and ^{31}P chemical shifts are referenced to external H_3PO_4 (85%). UV–visible spectra were obtained on a Perkin-Elmer Lambda 18 spectrophotometer, and FT-IR spectra on a Nicolet 510 spectrometer in 0.1 mm CaF_2 solution cells.

Kinetic Measurements. ^1H NMR Experiments. Sample preparation was carried out as follows: complex $[(\eta^6\text{-}p\text{-cymene})\text{RuCl}(\text{PCy}_3)][\text{X}]$ (**8**, 3–12 mg) and the propargylic alcohol $\text{HC}\equiv\text{CC}(\text{OH})\text{Ar}_2$ (1.1 equiv, 1–6 mg) were weighed directly into a 5 mm NMR tube. After two vacuum-argon cycles, benzene- d_6 or dichloromethane- d_2 (550 μL) was added using a microsyringe. The tube was sealed under argon with a rubber septum and shaken vigorously to ensure complete dissolution of the starting

materials. Test experiments performed by ^{31}P NMR indicated conversion of complex **8** into the corresponding allenylidene complex **4** after 15–20 min at room temperature. *N,N*-Diallyltosylamide **7** was then added and the tube sealed under argon with a rubber septum, without mixing. For the experiments in the presence of HBF_4 , a 7.5 M solution of the acid in diethyl ether (Aldrich) was introduced by microsyringe before the addition of the olefin. The sample was shaken vigorously just before introduction into the NMR probe, thermostated at the desired temperature. After a few minutes for thermal equilibration and experiment setup, a series of spectra were collected at regular interval times using a macrosequence of the NMR software. Diene **7** and product concentrations were calculated by integrating the allylic methylene signals at δ 3.7 (d, $J = 6.2$ Hz) and 4.0 ppm, respectively, vs the methyl signal of the tosyl group at 2.3 ppm, as internal standard. The zero-order rate constants, k_0 ($\text{mol L}^{-1} \text{s}^{-1}$), of the reactions in dichloromethane- d_2 were determined from the plots of [7] vs time, which exhibited a linear dependence up to about 100 min reaction time ($k_0 = \text{slope}$).

UV–visible Measurements. Complex **8** (3–6 mg), the propargylic alcohol (1.1 equiv), and 2 mL of the solvent were introduced under argon into a 10 mL volumetric flask, which was then shaken to ensure dissolution of the starting materials. The formation of the desired allenylidene complex was indicated by the intense ruby color of the solution and occasionally controlled by ^{31}P NMR. After 15 min, the volumetric flask was brought to volume by addition of either benzene or dichloromethane. The sample was further diluted to the desired concentration range ($(1\text{--}5) \times 10^{-5}$ M), and the measurements were performed immediately afterward, by recording a series of spectra or by following absorbance at fixed wavelengths. Data of absorbance vs time were fitted by nonlinear least-squares regression analysis of the first-order rate equation, which yields values of k_{obs} and A_∞ (eq 1).

$$A_t = A_\infty + (A_0 - A_\infty) \exp - (k_{\text{obs}}t) \quad (1)$$

Acknowledgment. The authors are grateful to Institut Universitaire de France (P.H.D.) and to the European Network IDECAT.

Supporting Information Available: $^{31}\text{P}\{^1\text{H}\}$ NMR spectrum of the reaction solution of complexes **8** and $(\text{Ph})_2\text{C}(\text{OH})\text{C}\equiv\text{CH}$, representative kinetic plots of the RCM reaction of **7**, and Eyring plot of the allenylidene–indenylidene rearrangement of complexes **4a** and **4e**. This material is available free of charge via the Internet at <http://pubs.acs.org>.